AIP Journal of Applied Physics

Ionoluminescent response of several phosphor screens to keV ions of different masses

D. Jiménez-Rey, B. Zurro, G. García, A. Baciero, L. Rodríguez-Barquero, and M. García-Munoz

Citation: Journal of Applied Physics **104**, 064911 (2008); doi: 10.1063/1.2979327
View online: http://dx.doi.org/10.1063/1.2979327
View Table of Contents: http://scitation.aip.org/content/aip/journal/jap/104/6?ver=pdfcov
Published by the AIP Publishing

Ionoluminescent response of several phosphor screens to keV ions of different masses

D. Jiménez-Rey,[1,a)] B. Zurro,[1] G. García,[2] A. Baciero,[1] L. Rodríguez-Barquero,[3] and M. García-Munoz[4]
[1]*Laboratorio Nacional de Fusión, Asociación Euratom-CIEMAT, Av. Complutense 22, E-28040 Madrid, Spain*
[2]*Instituto de Matemáticas y Física Fundamental, Consejo Superior de Investigaciones Científicas, Serrano 113-bis, 28006 Madrid, Spain*
[3]*Laboratorio de Metrología de Radiaciones Ionizantes, CIEMAT, Av. Complutense 22, E-28040 Madrid, Spain*
[4]*Max-Planck-Institut für Plasmaphysik, EURATOM Association, Boltzmannstr. 2, Garching D-85748, Germany*

(Received 23 October 2007; accepted 21 July 2008; published online 24 September 2008)

We have characterized the ionoluminescent response of several phosphor powder materials when irradiated with ions of different masses (H^+, He^+, Ar^+) accelerated to keV energies. In particular, we have determined the absolute luminosity in terms of the number of photons per incident ion emitted by luminescent screens of Y_2O_2S:Tb (P45), $Y_3Al_5O_{12}$:Ce (P46), Y_2SiO_5:Ce (P47), Y_2O_3:Eu (P56), and $SrGa_2S_4$:Eu (TG-green). Their ionoluminescence has been studied as a function of ion beam energy and current and ion fluency. The energy trend and mass dependence of selected experimental results are compared relative to stopping and range of ions in matter (SRIM) code predictions. © *2008 American Institute of Physics*. [DOI: 10.1063/1.2979327]

I. INTRODUCTION

Ionoluminescence (IL) is nonthermal light emission induced by the bombardment of materials with accelerated ions. It can be pictured as a de-excitation of a previously stimulated electronic system, related either to valence electrons of particular atoms (extrinsic luminescence) or to defects inside crystalline structures (intrinsic luminescence).[1] Its main use is for identification of impurities or detection of structural defects inside modern synthetic materials. In contrast, this work is motivated by the need to identify scintillator materials for detecting fast ion losses from magnetically confined fusion plasmas. Indeed, scintillator based detectors are well suited for this purpose due to their immunity to electromagnetic interference and ground loops, as well as to their compactness.[2,3]

For this purpose, screens made of luminescent material must exhibit a known response, reasonable linearity, and sensitivity to accelerated charged particles. At present, a broad range of powder luminescent materials is available with emissions at different visible wavelengths and with different response times. However, although their efficiencies to vacuum ultraviolet (VUV) radiation, x-ray photons, and electrons have been studied extensively, their behavior to accelerated ions, in the energy range of interest for fast ion-loss detectors in fusion plasmas, is unknown. This limitation has constrained the use of this type of detector to applications that do not require the ionoluminescent response of the screen as a function of energy, such as the correlation of neutral beam injection ions escaping with magnetohydrodinamic plasma activity.[4,5] However, knowledge of the luminescent material response as a function of ion beam energy opens avenues for the application of this type of detector.

This work is primarily motivated by the requirement to develop a fast ion-loss diagnostic probe for the TJ-II stellarator.[6–9] To back up this development, we have studied the light response of several phosphor screens under bombardment by different ions with energies ≤ 33 keV. Such a study will allow us to choose the most appropriate phosphor for work as the ion-photon converter in this fast ion-loss detector. In order to quantify the fast ion flux intercepted by the diagnostic ion probe, it is necessary to determine the absolute luminosity of its screen for such ions. Here, absolute IL measurements, in terms of photons emitted per incident ion, are presented for four candidate materials. The materials were selected according to their availability, radiation hardness for particular conditions, fast response, and prior use in plasma diagnostics for radiation monitoring. These are Y_2O_2S:Tb (P45), $Y_3Al_5O_{12}$:Ce (P46), Y_2SiO_5:Ce (P47), and Y_2O_3:Eu (P56).[10,11] Two reference screens have also been selected: a commercially available crystal scintillator screen $Y_3Al_5O_{12}$:Ce [also known as YAG:Ce (yttrium aluminum garnet) or P46 crystal],[12] and a $SrGa_2S_4$:Eu (TG-green) screen (deposited by a different method to that employed here) that has been used in another fusion experiment.[13,14]

In this paper, the experimental setup, the measurements made using H, He, and Ar ions at discrete energies between approximately 1 keV and approximately 33 keV, and the data analysis employed are described first. Next, quantitative results are summarized and used to estimate luminescent efficiencies (i.e., measured as the number of photons per MeV of incident ion energy). Finally, the suitability of the materials for the application outlined previously, and similar applications, are discussed.

a)Electronic mail: d.jimenez@ciemat.es.

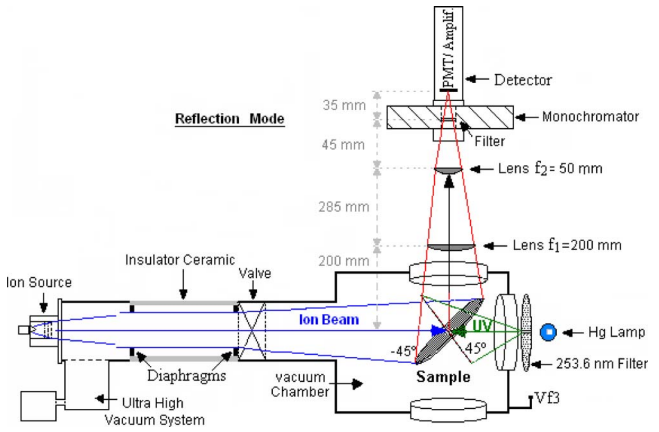

FIG. 1. (Color online) A schematic diagram of the experimental setup showing the different elements used to excite luminescence of the sample, either ions (blue, from left side) or UV light (green, right side). The luminescence is measured by a very sensitive system composed of a scan filter monochromator (400–700 nm), and a photomultiplier.

II. EXPERIMENTAL SETUP

The IL measurements presented were made at the Optics and Spectroscopy Laboratory of the *Laboratorio Nacional de Fusión por Confinamiento Magnético* at CIEMAT, Madrid, Spain. The experimental setup developed to perform these measurements is shown in Figs. 1 and 2. The system is composed of the following elements: (1) an ion source, with its power supply and vacuum system, (2) a Wien filter to select the ions, (3) a five-way vacuum chamber where the samples under study are located, (4) a spectral and detection system for ionoluminescent light, and (5) a Hg lamp for photoluminescence (PL). These are described in more detail below.

First, the ion beam for exciting IL is generated using a commercial ion source (model MPS-3000-FC by Ion Tech. Inc. Colorado). This source can be operated with different gases as required. The ion source needs slightly different tuning depending on the working gas; the latter is introduced, through the ion source head, and regulated by means of a micrometric valve. A tungsten cathode, which provides the electrons to ionize the gas, is located close to the gas injection. The typical operating parameters of the ion source were a nominal accelerating current of 1 mA and a nominal beam current of approximately 30 mA. Since the ion source parameters as well as the current filament are very sensitive to pressure variations, special care was needed to achieve good control of the gas inlet and power supply stability. Also,

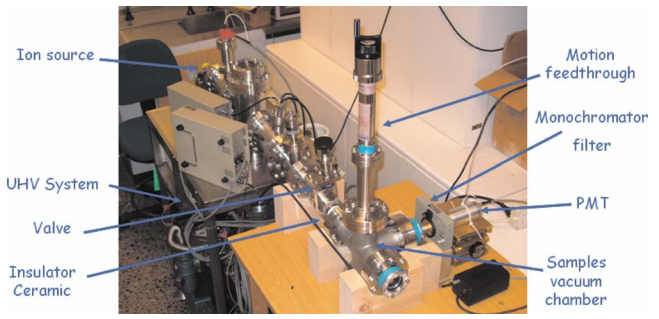

FIG. 2. (Color online) Photography of the facility to measure IL at the CIEMAT laboratory.

several hours of conditioning for the entire vacuum and ion source system was performed prior to performing measurements. The base pressure achieved in the system was $\leq 10^{-7}$ mbar and the typical working gas pressure was approximately 1.4×10^{-4} mbar.

Second, the ions created with the tungsten cathode are accelerated before passing through a 10 mm diameter collimated entrance slit into the Wien filter, which allows the passage of singly ionized ions only.[15] Finally, the ions are accelerated using a high-voltage power supply that provides the accelerating voltage of up to 33 keV (the system can be operated up to 60 keV). The bias voltage (V_{f3}) is applied to the five-way vacuum chamber (model CX5–63 by Caburn-MDC, UK), within which the luminescent materials under study are located. The target chamber is electrically insolated from the Wien filter and the rest of the device by a ceramic tube (see Fig. 1). In this way, current densities of up to 2.7×10^{-7} A cm^{-2} and ion fluxes of up to 1.73×10^{12} cm^{-2} s^{-1} can be achieved at the target.

Next, the screens under investigation are mounted in groups of up to six units in the five-way vacuum cross. The sample holder is attached to the end of a combined rotary and linear motion feedthrough (model VF-180–3 by Huntington, USA) that is located on the second way of the five-way cross.[16] This system permits measurements to be performed at different positions across each sample, see Fig. 1, as well as permits the angle with regard to the ion beam and the Hg lamp to be varied, i.e., with a sample set at −45° to the ion beam. PL (induced by a Hg ultraviolet lamp, model 6061, by Oriel, USA) of the sample can be performed to check the light emission spectrum of the sample.[17]

The luminescence analysis and detection system, mounted on the outside of a zero-length viewport located at the end of the third way, is used to measure the light emitted from the samples. Note that the luminescence light output is measured in reflection mode for both ions and UV light, i.e., from the side of the screen facing the incident ion beam with the sample set at −45° to this beam (see Fig. 1). In addition, a thin coating of colloidal graphite in water (Aquadag® 18% by Acheson, Plymouth, UK) had been applied to the inner walls of the chamber in order to minimize internal reflections while apertures, located between the sample and detection system, further reduce stray light.

As mentioned above, the ion beam crosses a ceramic tube, with two diaphragms to limit the beam to a diameter of 10 mm, which electrically isolates the ion source from the experimental chamber. Each diaphragm is set at the voltage corresponding to each of the two parts (ion source and five-way cross) in order to obtain a uniform field in this ion transport zone. The energy of the ions impinging on the luminescent screen can be varied by programming the voltage applied to the entire experimental chamber (V_{f3}), which is surrounded by a protective plastic shield for personal safety. While operation up to 10 keV does not present any serious difficulties, extending the range up to 33 keV is a more delicate task, since these screens are bad conductors and are prone to produce arcs.[18] This is aggravated by the fact that for ion detection the phosphor layer cannot be coated with a very thin layer of aluminum (which is usually done to avoid

charge accumulation on a phosphor surface for soft and hard x-ray detection), which is customarily connected to ground to suppress this space-charge effect. Here, this problem was overcome by placing a thin nickel grid, with a transparency of 80%, over the phosphor layer.

A. Spectral and detection system

The setup described allows luminescence to be excited by either UV radiation from the Hg lamp, after passing through a filter at 253.6 nm ($\Delta\lambda=1$ nm), or the ion beam. In the former case, only the most intense UV line is used to excite the luminescence, while the remaining lines emitted by the lamp cannot reach the spectral and detection systems through either reflection or scattering off the screen surface. The operation mode, IL or PL, is selected by rotating the position of the sample.

The spectral and detection systems are composed of collection optics, a continuous tunable interference filter, and a photomultiplier (see Fig. 1). The system consists of an optical set in front of a filter monochromator, covering the range between 400 and 700 nm (model 7155 by Oriel, USA), and a photomultiplier (model 5784–04 by Hamamatsu, Japan),[19] which has a current amplifier attached with a bandwidth of 20 kHz and a gain of 10^6 V/A. The optical set is formed by two plane-convex lenses with $f_1=200$ mm and $f_2=50$ mm; the first one is mounted close to the vacuum chamber, and the second one close to the monochromator input slit in such a way as to focus the IL light on the photocathode of the detector. The resultant spectral resolution is 20 nm when the filter monochromator is operated with a slit of 1 mm. Next, the intrinsic gain of the photomultiplier can be chosen by varying a continuous signal between 0 and 1 V supplied by a stabilized low voltage source applied to the integrated electronic package of the photomultiplier. This approach is more compact and has more throughput than an equivalent grating monochromator. In addition, the low resolution of the filter monochromator is more appropriate for this type of measurement, which needs poor spectral resolution but very high sensitivity. The sole drawback of this approach is the manual scan of the wavelength. However, for standard IL measurements the wavelength is fixed and tuned to the peak of the emission of the corresponding material. Now, the slit width can be adjusted for the particular luminescent material in order to obtain the maximum signal-to-noise ratio. Moreover, the filtering of the luminescent light is essential in order to optimize the signal-to-noise ratio since there are several sources of background light emission. These include the emission from the thermoelectric filament of the ion source cathode, which reaches the phosphor screen and is diffused by it toward the analysis-detection system, as well as weak line emissions from the ion beam. Indeed, background reduction is the most critical issue when measuring in the lowest energy ranges where signal levels can be comparable to the background level.

Finally, the determination of the absolute response of the filter monochromator was carried out using a spectrophotometer (model CARY 5E by Varian, USA), operated from 300 to 800 nm. Its response for a discrete set of wavelengths and for a slit of 1 mm was quantified by fitting its transmission curve by means of a Gaussian. The resulting transmission peaks and their full widths at half maximum (FWHM) are shown in Fig. 3 as a function of wavelength. The corresponding numerical results are given in Table I. These data are needed when processing raw data in order to obtain an absolute response of the phosphor screen IL, since the relation between the signal recorded by the data acquisition system and the ions impinging on a material is influenced by the response of all intermediate elements.

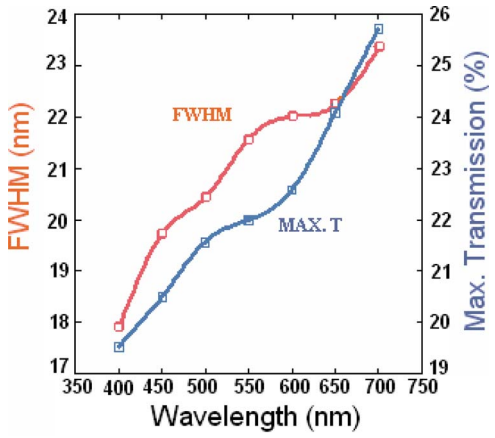

FIG. 3. (Color online) The transmission properties of the low resolution spectral system are shown by the variation in the instrumental width (FWHM, left axis) and in the relative transmission (right axis).

B. Alignment, adjustment, and operation

In the experimental facility described here, it is also possible to study the PL of the sample, using the same setup, by rotating the sample. This unique feature offers several additional advantages. First, it is possible to perform the optical alignment and the optimization of the measurements without bombarding the sample with ions. Second, it is possible to check the luminescence spectrum of the sample in its working position. Third, when the phosphor is deposited on a quartz plate—which is transparent to the radiation of the Hg lamp at 253.6 nm—luminescence can be excited through both sides of the sample, and consequently, it is possible to track any possible long term damage to the phosphor due to ion beam exposure.

TABLE I. Dependence of maximum transmission and FWHM of the filter monochromator as a function of wavelength.

λ (nm)	Transmission (%)	FWHM (nm)
400	19.539	17.89
450	20.495	19.72
500	21.566	20.42
570	21.990	21.56
611	22.573	22.00
650	24.078	22.22
700	25.713	23.33

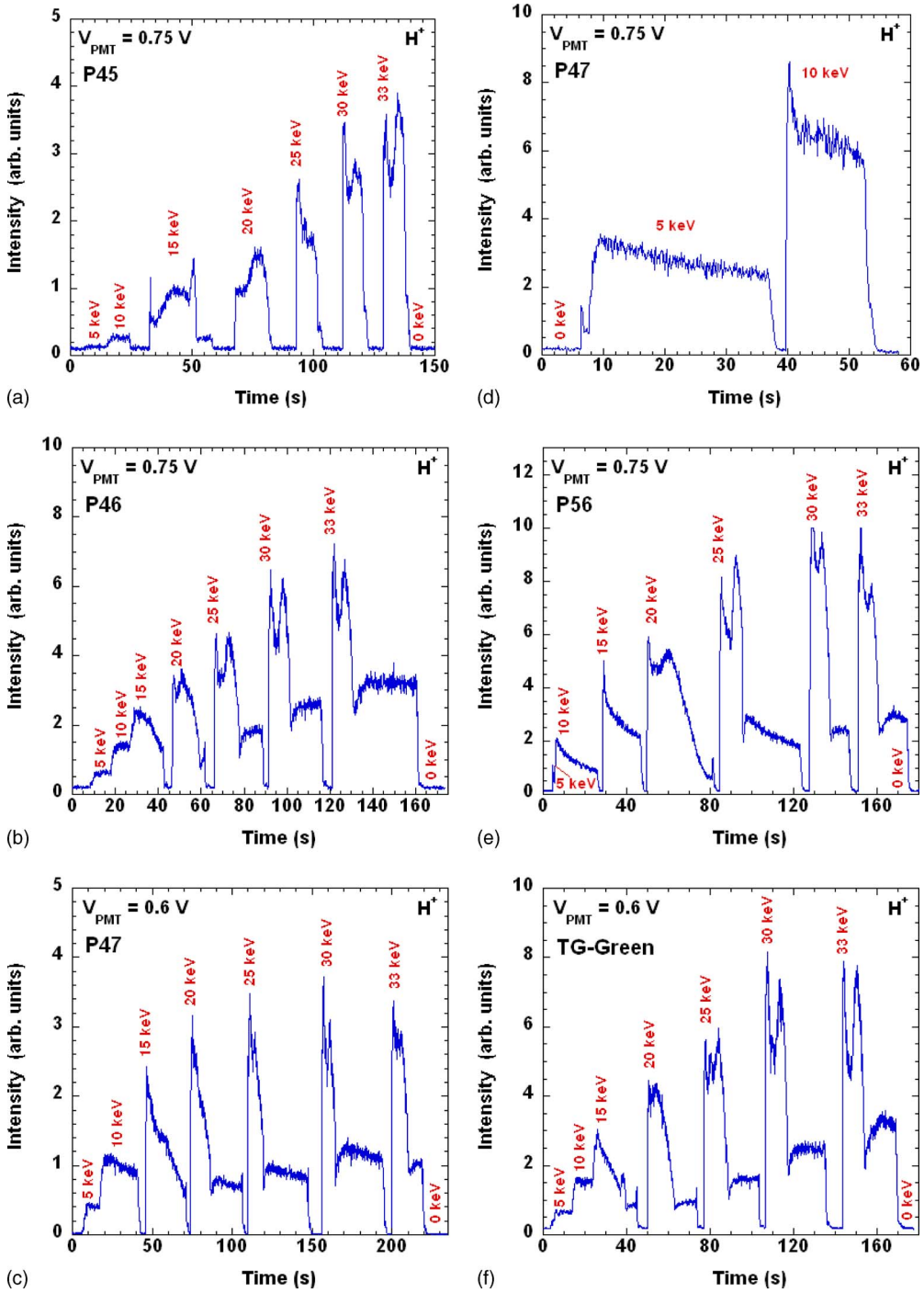

FIG. 4. (Color online) The time evolution of the raw ionoluminescent signal during several seconds of irradiation of the phosphor screen. Several steps in the ion beam energy are seen. When the bias is set to zero between the different biasing values, the signal recovers the background value: (a) P45, (b) P46, (c) P47, (d) P47 (expanded view) (e) P56, and (f) TG-green.

C. Data acquisition and processing

The output signals from the photomultiplier are fed, via a BNC connector, to a Universal Serial Bus (USB) converter box (Series 9800 by Data Translation, USA) attached to a laptop computer for storage. This system can also be operated as a standard oscilloscope, a very convenient feature in the checking phase (see Fig. 4).

Several steps were required when postprocessing the data. First, the ion beam flux incident on a sample was determined from the ion current density. The current reaching the sample varies typically between approximately 0.25 and 1×10^{-7} A. The number of photons emitted perpendicularly from the screen per steradian was calculated taking into account the geometry of the light collection. The observation geometry (see Fig. 1) is determined by the surface of the photomultiplier photocathode (diameter=8 mm), the distances between the luminescent screen, lenses, and monochromator input slit, and between the former and the photocathode (these are given in Fig. 1). The luminescent bright spot from the screen, which is set at 45° to the ion beam, is

TABLE II. List of materials prepared in-house (except TG-green) for IL measurements together with their most important properties.

Designation	Composition	Density (g/cm^3)	Emission peak (nm)	Activator density (%)	Decay time	Manufacturer
P45	$Y_2O_2S:Tb$	2.88	530	2	1.4 ms	Osram Sylvania
P46	$Y_3Al_5O_{12}:Ce$	4.15	540	2	0.16 μs	Phosphor Technology
P47	$Y_2Si_5O_{12}:Ce$	2.054	400	3	0.14 μs	Osram Sylvania
P56	$Y_2O_3:Eu$	4.8	611	4	1 ms	Osram Sylvania
TG-green	$SrGa_2S_4:Eu$	3.65	530	4	0.54 μs	Sarnoff Co.

approximated by an extended Lambertian source of diameter 10 mm. In this case, the fractional solid angle to the detector was obtained using equations described in Ref. 20 for disk sources which results in a fixed error of approximately 1% for absolute measurements.[18] Second, the photon fluxes reaching the photomultiplier were determined from the time integrated light signals using wavelength sensitivity curves provided by the manufacturer[19] after correcting for transmission losses in the vacuum window and for signal amplification (fixed at 1 $V/\mu A$).

The formula relating the signal delivered by the detector with the different sensitivity parameters of the experimental system is

$$V_{\text{output}} = R_{\text{ph}}^{\text{IL}} \Gamma R_{\text{PMT}}^{Vp} T_{\text{opt}} \Omega S, \tag{1}$$

where V_{output} (volts) is the signal from the detector, Γ [ions/cm^2 s] is the known flux provided by the ion source, that when operated with a current I, is given by $I/(S_B \times 1.6 \times 10^{-19})$ (ions/s), where S_B is the effective beam area. $R_{\text{ph}}^{\text{IL}}$[photons/(ions sr)] is the luminescence response to the ion bombardment, where R_{PMT}^{Vp}[V/(photons s)] is the photomultiplier response for a polarization of V_p. This is determined from the response in (V/nW) provided by the manufacture through the expression

$$R_{\text{PMT}}^{Vp} = 60.981 f_w (Vp)^{7.0857} / (5.034 \times 10^{15} \times \lambda \times 10^{-9}), \tag{2}$$

where f_W is the relative sensitivity of the photomultiplier tube normalized at a wavelength of 420 nm, and λ expressed in nm. T_{opt} is the optical transmission of the entire optical system, lenses, window, and filter spectrometer. It is determined by

$$T_{\text{opt}} = T_0 \int S_{\text{ionl}}(\lambda) T_{\text{fil}}(\lambda) d\lambda, \tag{3}$$

where S_{ionl} is the luminescent spectrum of the material, T_{fil} the spectral transmission curve of the filter monochromator, and T_0 the optical transmittance of window and lenses. Ω (sr) is the light collection solid angle, determined by the observation geometry. Finally, $S(cm^2)$ is the surface area bombarded by the ions.

From Eq. (1), the effective response of the luminescent screen $R_{\text{ph}}^{\text{IL}}$, is determined. When a screen is used for estimating the fast ion loss flux, the same formula must be used, but in that case Γ is the quantity to be determined.

III. LUMINESCENT MATERIALS AND SCREENS

The phosphor powder screens studied were prepared in-house from commercially available phosphor grains (except TG-green). Uniform screens, deposited on quartz or stainless steel plates, were prepared by a sedimentation method, similar to that previously used in Ref. 17 where it is explained in more detail. However, a change in the procedure described therein was required as the standard bonding material used for quartz plates (aluminum chloride) chemically attacks metallic surfaces and so was replaced by sodium dactyl sulfosuccianate ($C_{20}H_{37}O_7SNa$), in a concentration of 1.6%, for metallic plates. In addition to the screens prepared in this way, two additional luminescent screens were employed for reference purposes: one was provided by the ASDEX Upgrade (AUG) team, TG-green phosphor,[14] while the other is a commercially available YAG:Ce crystal scintillator screen, whose behavior under bombardment by radiation and particles is well documented.[12]

The selected materials and their properties are given in Table II together with their standard denomination according to the Joint Electron Devices Engineering Council[10] (except TG-green), their chemical compositions, densities, main emission peaks, activator densities concentrations, decay times, and manufacturers. The main characteristics of these materials are outlined below, but for more details the reader is referred to Refs. 10 and 11.

The behavior of several of these phosphor screens has been previously modeled and characterized for use as broadband x-ray and VUV detectors.[21] Moreover, several prototypes of broadband radiation detectors based on such screens are operative in the TJ-II stellarator.[22] An inspection of Table II demonstrates the reasons for selecting these screens. For instance, although P45 has a moderate time response, it has been quoted as being one of the most sensitive phosphors available for detecting VUV and soft x-ray radiation, when a fast response is not a key parameter. In contrast, P46 and P47 exhibit much faster luminescence response times. In the case of P45 it also has the advantage that it is possible to work up to and beyond 150 °C, which can be important for a detector probe operating close to a hot plasma.[16]

The first material in Table II is P45 ($Y_2O_2S:Tb$). The raw material to produce these screens was obtained from Osram Sylvania (Towanda, USA) in powdered form. It was deposited with a surface density of approximately 17.59 mg cm^{-2}. The luminescent centers are the Tb^{+3} ions uniformly distributed in the principal host lattice of the ma-

terial Y_2O_2S. It was selected for this experiment because it is the most sensitive phosphor when bombarded with electrons or x rays.

The second sample is P46 ($Y_3Al_5O_{12}$:Ce, also known as YAG:Ce powder). It was provided in powdered form, with an average grain size of 6.64 μm and a cerium molar concentration between 1% and 2%, by Phosphor Technology (Nazening, U.K.). Screens with a surface density of approximately 15.36 mg cm^{-2} are used in this work. The luminescent centers are the Ce^{+3} impurities uniformly distributed within the main host lattice of $Y_3Al_5O_{12}$.The Ce^{+3} ion substitutes the Y^{+3} ion in the place of the symmetry D_2 of the dodecahedron for eight O^{-2} ions in its corners. The luminescent emission arises from allowed transitions of energy levels $5d-4f$ of the Ce^{+3} ion. Its luminescence exhibits a wide peak at 540 nm,[21] and its luminescence lifetime is 0.16 μs. Previously, screens of this material were selected for detecting VUV and x-ray photons in detectors developed at CIEMAT for monitoring broadband radiation for high temperature plasmas.[22]

The third material is P47 (Y_2SiO_5:Ce). The raw material to produce the screens was obtained from Osram Sylvania (Towanda, USA) in powdered form. The luminescent centers are the Ce^{+3} ions uniformly distributed in the principal host lattice of the material Y_2SiO_5. Screens of surface density approximately 14.97 mg cm^{-2} were prepared. This luminescent material has the fastest response (0.14 μs) among those selected for this work. The emission color when excited by ions is blue/violet.

The fourth material studied was P56 (Y_2O_3:Eu), which was supplied in grains by Osram Sylvania (Towanda, USA). It was deposited with a surface density of approximately 14.05 mg cm^{-2}. Its luminescence is due to the transition $^5D_0-^7F$ of the impurity Eu^{+3}, with a molar concentration of 4%, within the configuration $4f^6$. Its band gap is 5.6 eV, the luminescence decay time is approximately 1 ms, and it has an efficiency of 87% under catholuminescence.[11] In addition, its luminescence spectrum is narrow and peaks at 611 nm. The standard applications of this material are the production of the color red in television screens and the detection of low energy x rays (note: in some contexts this material is designated as P22R).

IV. RESULTS AND DISCUSSION

The results are presented here with the aim of providing empirical criteria for selecting the optimum screen for the fast ion detector under development or for others based on similar principles and operating in a similar ion energy range. The phosphor screens have been studied as a function of energy for H^+, He^+, and Ar^+ ions. In addition, other relevant aspects for achieving a correct understanding of the detector operation have also been addressed, for instance, the influence of ion beam current, ion fluency, and kinetic behavior of its response, as well as the ionoluminescent spectra. These studies can contribute to understanding different individual and combined effects that influence the response of these materials for the application of interest here.

Since one of the main drawbacks reported for phosphor screens operating in highly accelerated (MeV) ion beams is radiation damage,[23] the first point is the time evolution of the phosphor screen response when bombarded by ions in the energy range $\leq$33 keV, in particular for times significantly longer than those of the TJ-II fast ion detector ($\leq$300 ms). This effect is well illustrated in Fig. 4, where the ion luminescent response of five screens is shown versus time for a set of bias voltage (beam energy) steps, where different energy values are separated by short periods of zero bias. It can be seen, most clearly at higher energy (15–33 keV), that their response exhibits a transient behavior during the first part of the excitation, reaching a plateau, followed by a slow and monotonic decrease in response.

An effect of this type never has been reported in the literature for IL measurements at such energies. However, smoother degradation effects have been reported and studied for cathodoluminescence (CL) of similar luminescence screens.[24] In the case of electron luminescence excitation, the relationship between I_a, the aged intensity of the phosphor, I_0, the initial phosphor intensity, and N, the number of electrons deposited per cm^2, is normally given by Pfahnl´s law,[25] where $I_a=I_0/(1+C_BN)$, and C_B is the burning parameter. Its reciprocal is the number of electrons needed to reduce the intensity of the luminescence to one-half of its initial value. For the case of ion-induced IL in scintillators, the degradation has been studied for MeV ions (see Ref. 26 where degradation, which is plotted versus ion fluence, is fitted by a sum of exponentials). However, no similar studies are known for powdered phosphor screens. The IL degradation reflected in the curves in Fig. 4 exhibit a kinetic behavior similar to that reported in Ref. 26 at low ion energies; however, it is much more complicated for ion energies greater than 20 keV. Its analysis and discussion is outside the scope of the present paper. However, it is important to keep in mind this effect when using such screens for fast ion detection in plasma machines with long pulse duration and/or with ion fluences similar to those used in this work.

In consequence, in the following discussions, the response at a given energy is defined as the average value monitored during the first part of the excitation. When used as an ion-light converter in a fast ion detector for a short plasma discharge, the time interval for ion exposure is much shorter than the time displayed in Fig. 4. However, one must be aware of the complicated response that a material of this kind can have to ions bombarding its surface in a continuous manner or during long plasma discharges.

One important feature observed during the study of the IL spectra of the different screens, which is more pronounced under bombardment by a heavy ion such as argon, is the energy dependence of the ionoluminescent spectra. This must be taken into account when detecting low energy ions by this method, for instance, when selecting a broadband filter for rejecting background light from the plasma itself. In Fig. 5 we have plotted for Ar^+, the variation in the ionoluminescent spectra with ion beam energy for P45, P46, and P56 in the spectral range between 400 and 700 nm covered by the filter monochromator. These detailed spectra may help to understand the low energy behavior observed in the energy scan data of some screens. A comparison of IL and PL

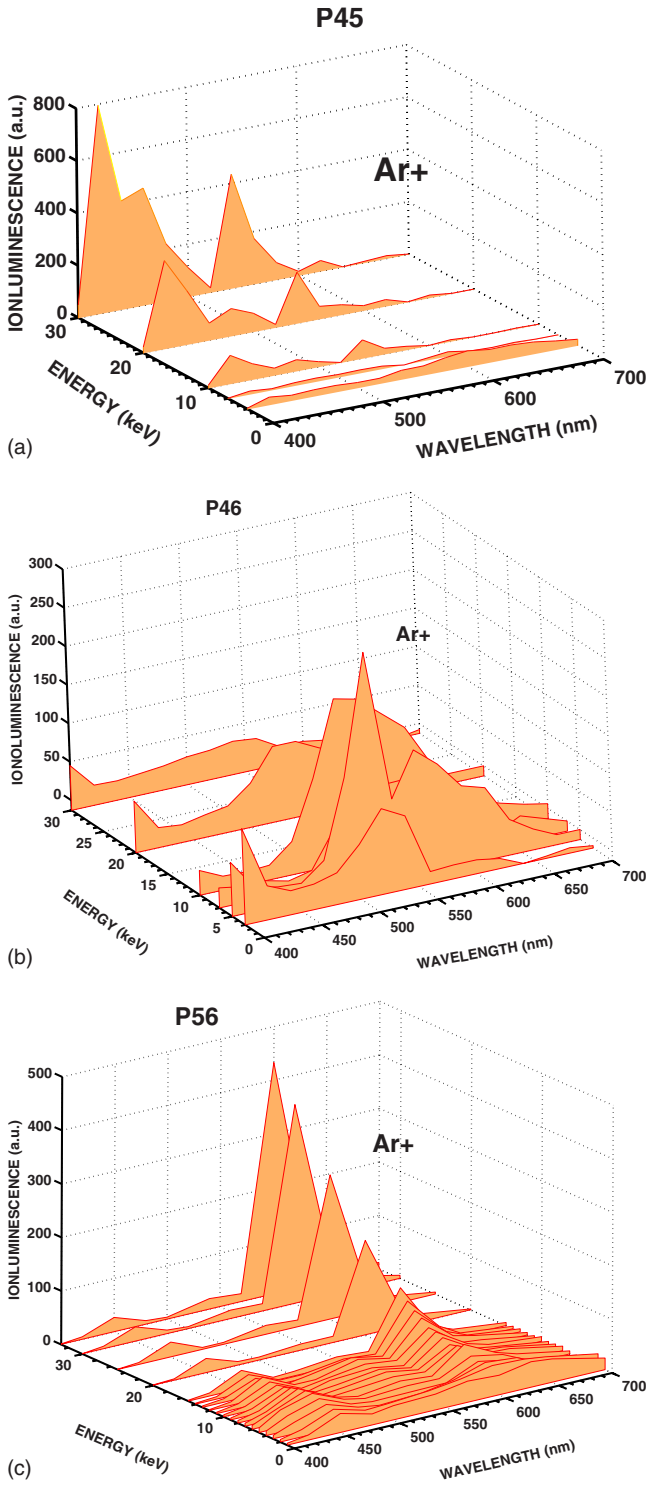

FIG. 5. (Color online) A selection of plots corresponding to ionoluminescent spectra, in the range covered by the spectrometer, obtained at discrete energies of the ion beam (Ar) for representative phosphors: (a) P45, (b) P46, and (c) P56.

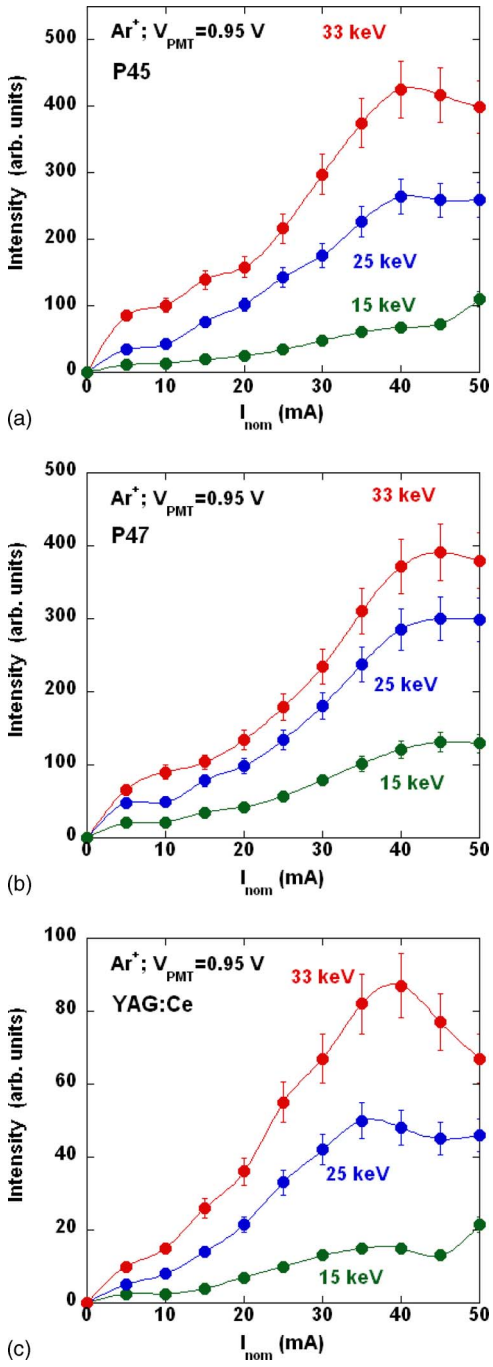

FIG. 6. (Color online) Influence of the ion beam current for three discrete energies of the ion beam (15, 25, and 33 keV) on (a) P45, (b) P47, and (c) YAG:Ce crystal. A clear saturation of the response is evident for current values above 35–40 mA.

spectra permits identification of the spectral features that can be ascribed to ion-induced defects in the material. In early works, the phenomenon of luminescence induced by the impact of a keV energy ion on alkali halides was connected with the presence of contaminants in the crystal. Presently, it is believed that the origin of the light emission is radiation defects,[27] and therefore this phenomenon can be useful not only for surface studies but also for particulate dosimetry.

Next, a series of experiments has been performed in which the ion beam current has been systematically varied while monitoring the IL. This was done to evaluate the influence of the ion beam intensity on the IL response of the phosphor screens at discrete energies. The results of current scans carried out on three phosphor screens for three values of the ion beam acceleration voltage are plotted in Fig. 6. These curves demonstrate a clear saturation with beam current as nominal values beyond 35–40 mA are reached. For this reason, systematic studies of IL versus ion beam energy, presented in the following section, have been restricted to

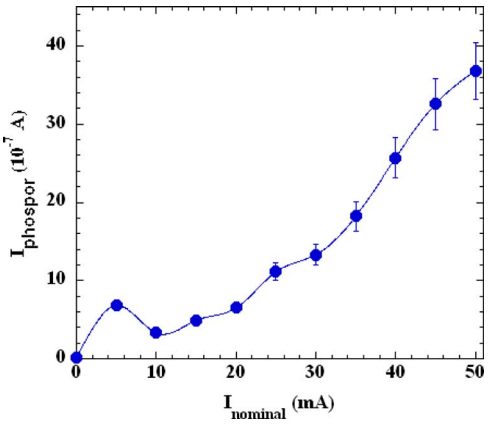

FIG. 7. (Color online) Plot of the actual current measured at sample position vs the nominal current of the ion source provided by its own control system.

nominal currents not greater than 30 mA. Next, in Fig. 7 the relationship between the nominal current of the ion source, measured at the head, and the actual current reaching the sample is considered. It is seen here that the linear behavior of IL signal with ion current is limited to a narrow range of ion current (<0.1 μA) impinging on the phosphor screen. An IL model developed and tested for experiments performed at many energies,[28] significantly higher than those reported here, has introduced the idea of a maximum electron energy deposition density, above which saturation of luminescence centers occurs; this effect could also be present here as revealed by these current scan data. This limitation must be taken into account when using such screens to monitor ion flux at the edge of plasma machines.

The key property of a luminescent material, from the point of view of its use for detecting fast ions in fusion plasmas, is its luminescent response to the energy of the ions impinging on it, (it is desirable that the detector can discriminate between ions having different energies). In addition, the relative response of different materials to ion beam energy can be used to identify which is the most convenient choice for our application. In Fig. 8, the IL response of the selected phosphor screens to protons is shown. This is one of the most

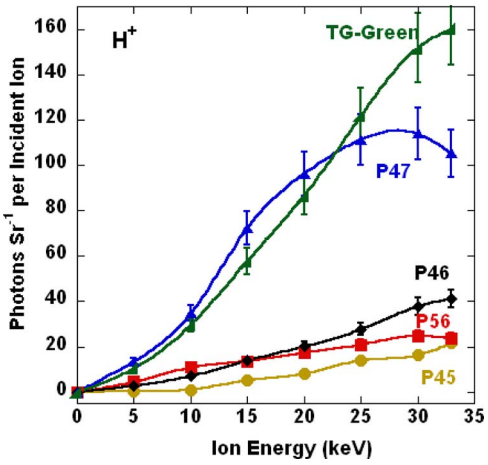

FIG. 8. (Color online) The IL response as a function of the proton beam energy for all the phosphor screens studied. A slight saturation effect is seen at the highest energy values, which is more pronounced for the case of the P47 screen.

TABLE III. A comparison of IL light production by H^+ irradiation (in absolute values) with normalized values for CL and PL for the materials under study. In the case of P45 its relative CL efficiency is high compared to the other materials. However, its relative IL efficiency is low. On the other hand, the relative response of P47 is higher for IL.

	IL H^+ up to $\leq$33 keV (photons MeV^{-1})	CL e^- up to 33 keV (normalized)	PL UV up to 253.6 nm (normalized)
P45	2100	1	0.150
P46	4100	0.123	0.027
P47	11680	0.150	0.043
P56	2340	0.998	1
TG-green	16504	···	0.336

interesting IL data not only for the application outlined here but also for similar applications in other plasma fusion devices, see Table III (IL). A highlight from Fig. 8 is the good response of the TG-green screen, which has been used by the AUG group[14] in a fast ion detector. Since the TG-green screen is a commercial screen (by Sarnoff Co.), and has been prepared by a proprietary method, it is not possible to determine whether its enhanced response is due exclusively to the intrinsic phosphor response or whether the deposition method plays a role. In the future, a sample of this phosphor deposited by an in-house developed method will be tested in order to elucidate this uncertainty. Indeed, the phosphor deposition method has been quoted as being an important factor for a phosphor response when applied to detect radiation. Moreover, the IL dependence with ion mass can be understood because the energy loss rate, for weakly penetrating particles, increases with particle mass[11] [see Table IV (stopping range)]. For instance this can be seen in the Fig. 9, for particles with the same energy incident on the P45 screen, where a He^+ ion produces approximately 0.7 times the light produced by a H^+ ion while an Ar^+ ion produces approximately 0.11 times the light produced by the H^+ ion.

Next, a relative comparison is made between the evolution of IL, measured as a function of accelerated particle mass, and IL predicted by a code. For this, the relationship between light output and the linear energy transfer of the ion beam, obtained using the stopping and range of ions in matter (SRIM) code,[29] was used. For this, surface effects, nonradiative effects, and nuclear collisions [atom/atom elastic collisions (nuclear component of the stopping range)] were not considered, so this is a close approximation to the total energy of the incident particle going into inelastic light-

TABLE IV. Estimated stopping ranges of accelerated argon, hydrogen and helium ions with 35 keV in the phosphors under study. For this, 10000 ions were used in the simulations.[28]

Designation	Stopping range (Å) Ar^+	H^+	He^+
P45	505	4309	3532
P46	294	2834	2108
P47	557	5235	4180
P56	312	2919	2189
TG-green	445	3127	3011

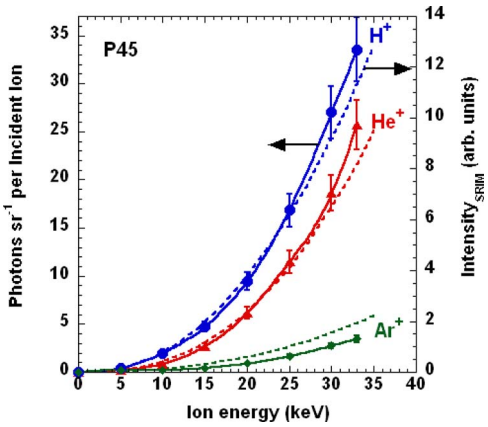

FIG. 9. (Color online) Absolute IL response of P45 as a function of incident ion beam energy for three different ions (continuous lines) and theoretical estimates of the same, using a first approximation based on the SRIM code (dotted lines). Good correlation is seen for all ions at low energies ($\leq$25 keV).

producing processes in the crystal. Thus, following this procedure and integrating the energy loss in the inelastic process $[(dE/dx)e]$, the broken curves shown in Fig. 9 were obtained. It can be seen from this figure that the relative evolutions of IL as a function of energy are in good agreement for all the ions with their experimental curves up to approximately 25 keV. At higher energies, a discrepancy becomes notable. This may suggest that a more complex model is needed.

In Fig. 9, the measured response of the representative phosphor screen, i.e., P45, which was used in the initial prototype of the fast ion detector for the TJ-II device, is shown for the three types of ions used in this work; a similar dependence has been found for the other phosphor screens studied. For illustration purposes the results of a similar study carried out with the crystal scintillator screen, YAG:Ce, are shown in Fig. 10. A comparison of these results permits the conclusion that a similar mass dependence is exhibited by both materials. Since both results are displayed on the same scale, it is apparent that the powder phosphor screen has a superior response compared to the crystalline one. Thus, although the latter material has several advantages, e.g., it is a popular and widely studied scintillator, it has a higher radiation damage threshold, and it is commonly used to monitor beam profiles in many laboratories, its low IL response, compared to the P45, makes it a second choice material for the application considered here, i.e., at low ion energies.

Finally, during ion irradiation of the screens their light output was seen to reduce gradually with time (Note: the same protocol was followed for all the materials). After several hours of irradiation, a dark coloring was clearly observed on the surface. It is thought that this is related to changes in the charge state of previously existing defects. These bands can have an important effect on absolute IL due to increased absorption. In other materials such as ceramics, a partial recovery of IL is observed if the sample is left at room temperature for some time after irradiation.[30] However, this was not observed here. It is known that the recovery

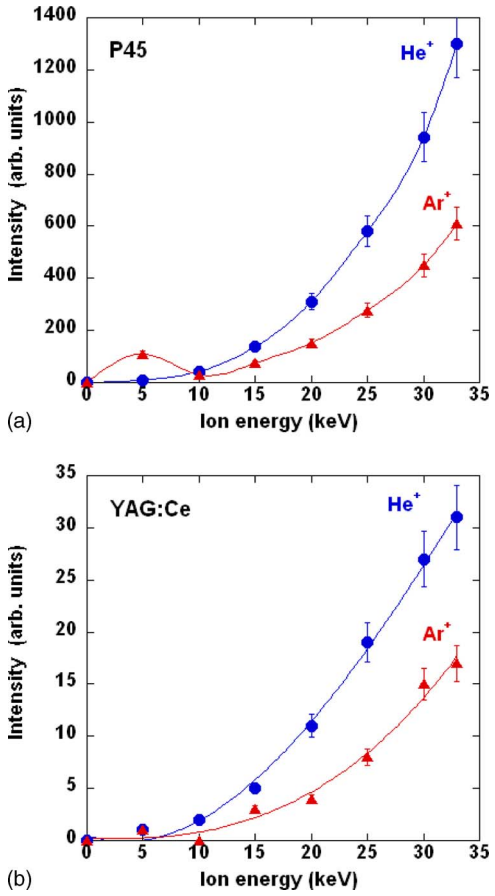

FIG. 10. (Color online) Comparative response of (a) a powdered screen made of P45 phosphor and (b) a crystal scintillator YAG:Ce. The results correspond to luminescence data obtained with He^+ and Ar^+ ions and plotted in the same relative scale to highlight the excellent response of the phosphor screen compared with the scintillator in this low energy range.

process may be accelerated by heat annealing or by ultraviolet light. Such recovery processes are considered for future evolutions of phosphor screen

V. CONCLUSIONS

The use of an optimized detection system with spectral resolution, based on a filter monochromator and a photomultiplier detector, has allowed us to perform IL measurements in the low energy range of interest to back up the design of a fast ion loss detector in medium sized plasma devices. It is expected that this IL data will be of great interest for ion beam detectors.

Several interesting aspects of the response of phosphor screens when they are used in fast ion detectors have been illustrated with data obtained in this facility. The transient response at the beginning of its excitation as well as its saturation with currents must be taken into account, not only when quantifying its relative response but also when considering its application. The relative response of selected luminescent materials as a function of the energy and mass of the bombarding ions has been studied and reported to support the development of fast ion detector design.

The behavior of several luminescent materials was studied under ion beam irradiation for energies below 35 keV. These measurements aid in the assessment of which are the

most appropriate materials used as very local fast ion detectors in the TJ-II device. The most sensitive materials studied were the TG-green and P47, although other materials exhibiting a smaller response present a better linearity with energy in this range. In addition, the absolute ionoluminescent efficiency of several materials for H^+, He^+, and Ar^+ ions of up to 33 keV have been determined; it is anticipated that these measurements will enable us to estimate ion losses in the TJ-II device.

ACKNOWLEDGMENTS

The authors thank Dr. K. J. McCarthy and Dr. E. Hollmann for a critical reading of the manuscript and English corrections. This work was partially funded by the Spanish "Ministerio de Educación y Ciencia" (MEC) under Grant No. FTN2003-0905 and D.J.R. is supported by a scholarship (Grant No. BES-2004-4771).

[1]D. Ghose and R. Hippler, in *Luminescence of Solids*, edited by D. R. Vij (Plenum, New York, 1998).
[2]M. Isobe, D. S. Darrow, T. Kondo, M. Sasao, K. Toi, M. Osakabe, H. Shimizu, Y. Yoshimura, C. Takahashi, S. Murakami, S. Okamura, and K. Matsuoka, Rev. Sci. Instrum. **70**, 827 (1999).
[3]D. S. Darrow, A. Werner, and A. Weller, Rev. Sci. Instrum. **72**, 2936 (2001).
[4]T. Kondo, M. Isobe, M. Sasao, D. S. Darrow, K. Toi, M. Takechi, M. Osakabe, Y. Yoshimura, C. Takahashi, S. Nishimura, G. Matsunaga, S. Okamura, K. Matsuoka, and CHS Group, Nucl. Fusion **40**, 1575 (2000).
[5]M. García-Muñoz, H.-U. Fahrbach, S. Günter, V. Igochine, M. J. Mantsinen, M. Marasaschek, P. Martin, P. Piovesan, K. Sassenberg, and H. Zohm, Phys. Rev. Lett. **100**, 055005 (2008).
[6]C. Burgos, B. Zurro, J. Guasp, M. A. Ochando, K. J. McCarthy, F. Medina, A. Baciero, M. Liniers, and C. Fuentes, Rev. Sci. Instrum. **74**, 1861 (2003).
[7]E. Ascasíbar, C. Alejaldre, J. Alonso, L. Almoguera, A. Baciero, R. Balbín, M. Blaumoser, J. Botija, B. Brañas, E. de la Cal, A. Cappa, J. Castellano, R. Carrasco, F. Castejón, J. R. Cepero, C. Cremy, J. Doncel, S. Eguilior, T. Estrada, A. Fernández, C. Fuentes, A. García, I. García-Cortés, J. Guasp, J. Herranz, C. Hidalgo, J. A. Jiménez, I. Kirpitchev, V. Krivenski, I. Labrador, F. Lapayese, K. Likin, M. Liniers, A. López-Fraguas, A. López-Sánchez, E. de la Luna, R. Martín, L. Martínez-Laso, M. Medrano, P. Méndez, K. J. McCarthy, F. Medina, B. van Milligen, M. Ochando, L. Pacios, I. Pastor, M. A. Pedrosa, A. de la Peña, A. Portas, J. Qin, L. Rodríguez-Rodrigo, J. Romero, A. Salas, E. Sánchez, J. Sánchez, F. Tabarés, D. Tafalla, V. Tribaldos, J. Vega, and B. Zurro, Fusion Eng. Des. **56–57**, 145 (2001).
[8]J. Guasp, M. Liniers, C. Fuentes, and G. Barrera, Fusion Technol. **35**, 32 (1999).
[9]J. Guasp and M. Liniers, Fusion Technol. **34**, 251 (1993).
[10]S. Shionoya and W. M. Yen, *Phosphor Handbook* (CRC, Boca Raton, 1999).
[11]G. Blasse and B. C. Grabmaier, *Luminescent Materials* (Springer, Berlin, 1994).
[12]T. Ludziejewski, M. Moszynski, M. Kapusta, D. Wolski, W. Klamra, and K. Moszynska, Nucl. Instrum. Methods Phys. Res. A **398**, 287 (1997).
[13]S. Yang, C. Stoffers, F. Zhang, S. M. Jacobsen, B. K. Wagner, and C. J. Summers, Appl. Phys. Lett. **72**, 158 (1998).
[14]M. García-Muñoz, P. Martin, H.-U. Fahrbach, M. Gobbin, S. Günter, M. Maraschek, L. Marrelli, and H. Zohm, and the ASDEX Upgrade Team, Nucl. Fusion **47**, L10 (2007).
[15]J. H. Moore, C. C. Davis, and M. A. Coplan, *Building Scientific Apparatus* (Westview, Colorado, 2002).
[16]A. Baciero, K. J. McCarthy, M. A. Acedo, L. Rodriguez-Barquero, J. Avila, Y. Huttel, V. Perez-Dieste, M. C. Asensio, and B. Zurro, J. Synchrotron Radiat. **7**, 215 (2000).
[17]B. Zurro, M. A. Ochando, A. Baciero, K. J. McCarthy, F. Medina, A. López-Sánchez, D. Rapisarda, D. Jimenez-Rey, A. Fernandez, I. Pastor, and J. Herranz, Rev. Sci. Instrum. **75**, 4231 (2004).
[18]K. J. McCarthy, J. García López, D. Jiménez-Rey, B. Zurro, A. Ibarra, A. Baciero, and M. A. Respaldiza, J. Nucl. Mater. **340**, 291 (2005).
[19]K. K. Hamamatsu Photonics, Photosensor Module H5783 Series, Technical Data Sheet (TPMHB0293EA), Shizuoka-ken, Japan, 1996.
[20]N. Tsoulfanidis, *Measurement and Detection of Radiation*, McGraw-Hill Series in Nuclear Engineering (Hemisphere, Washington, 1983).
[21]A. Baciero, "Caracterización cuantitativa de detectores luminiscentes para plasmas de fusión," Ph.D. thesis, Universidad Complutense de Madrid, 2004.
[22]B. Zurro, C. Burgos, K. J. McCarthy, and L. Rodriguez-Barquero, Rev. Sci. Instrum. **68**, 680 (1997).
[23]W. A. Hollerman, J. H. Fisher, G. A. Shelby, L. R. Holland, and G. M. Jenkins, IEEE Trans. Nucl. Sci. **38**, 184 (1991).
[24]H. C. Swart, T. A. Trottier, J. S. Sebastian, S. L. Jones, and P. H. Holloway, J. Appl. Phys. **83**, 4578 (1998).
[25]A. Pfahnl, *Advances in Electron Tube Techniques* (Pergamon, New York, 1961), p. 204.
[26]D. Broggio, J. M. Jung, R. Barillon, and T. Yamauchi, Radiat. Meas. **40**, 736 (2005).
[27]M. Suchanska, A. I. Bazhin, and E. I. Konopelko, Phys. Status Solidi B **182**, 231 (1994).
[28]K. Michaelian and A. Menchaca-Rocha, Phys. Rev. B **49**, 15550 (1994).
[29]J. M. Ziegler, http://www.srim.org/
[30]D. Jiménez-Rey, B. Zurro, K. J. McCarthy, G. García, and A. Baciero, Rev. Sci. Instrum. **79**, 1 (2008).